HHS Public Access

Author manuscript

Int J Dev Neurosci. Author manuscript; available in PMC 2019 November 01.

Published in final edited form as:

Int J Dev Neurosci. 2018 November ; 70: 25–33. doi:10.1016/j.ijdevneu.2018.05.006.

Ontogeny of white matter, toll-like receptor expression, and motor skills in the neonatal ferret

Jessica M. Snyder[a,1], **Thomas R. Wood**[b,1], **Kylie Corry**[b], **Daniel H. Moralejo**[b], **Pratik Parikh**[b], and **Sandra E. Juul**[b,*]

[a]Department of Comparative Medicine, University of Washington, Seattle, WA, United States

[b]Department of Pediatrics, University of Washington, Seattle, WA, United States

Abstract

Inflammation caused by perinatal infection, superimposed with hypoxia and/or hyperoxia, appears to be important in the pathogenesis of preterm neonatal encephalopathy, with white matter particularly vulnerable during the third trimester. The associated inflammatory response is at least partly mediated through Toll-like receptor (TLR)-dependent mechanisms. Immunohistochemistry, gene expression, and behavioral studies were used to characterize white matter development and determine TLR3 and TLR4 expression and accumulation in the neonatal ferret brain. Expression of markers of white matter development increased significantly between postnatal day (P)1 and P10 (NG2, PDGFRα) or P15 (Olig2), and either remained elevated (NG2), or decreased again at P40 (PDGFRα, Olig2). Olig2 immunostaining within the internal capsule was also greatest at P15. Myelin basic protein (MBP) immunostaining and mRNA expression increased markedly from P15 to P40 and into adulthood, which correlated with increasing performance on behavioral tests (negative geotaxis, cliff aversion, righting reflex, and catwalk gait analysis). TLR4 and TLR3 positive staining was low at all ages, but TLR3 and TLR4 mRNA expression both increased significantly from P1 to P40. Following lipopolysaccharide (LPS) and hypoxia/hyperoxia exposure at P10, meningeal and parenchymal inflammation was seen, including an increase in TLR4 positive cells. These data suggest that the neuroinflammation associated with prematurity could be modeled in the newborn ferret.

Keywords

Prematurity; White matter injury; Development; Brain; Central nervous system

1. Introduction

Up to fifty percent of surviving infants born extremely preterm (less than 28 weeks of gestation) develop long-term neurodevelopmental impairments affecting cognition and learning, or motor problems such as cerebral palsy (Scafidi et al., 2009). Inflammation caused by prenatal or postnatal infection, coupled with superimposed hypoxia and/or

*Corresponding author at: Department of Pediatrics, Division of Neonatology, Box 356320, HSB RR-542, Seattle, WA 98195, United States. sjuul@u.washington.edu (S.E. Juul).

[1]Contributed equally

hyperoxia, appears to be important in the pathogenesis of preterm neonatal encephalopathy (Back and Rosenberg, 2014; Volpe, 2009; Hagberg et al., 2015; Brehmer et al., 2012; Dean et al., 2015). This inflammatory response is at least partly mediated through Toll-like receptor (TLR)-dependent mechanisms (Thomson et al., 2014). White matter is particularly vulnerable to inflammation and hypoxia during the third trimester, and encephalopathy of prematurity is characterized by injury that can range from focal or multifocal cystic necrosis of the periventricular white matter to more diffuse, noncystic white matter injury (WMI), and abnormalities in myelination (Back, 2006). As preterm brain injury primarily involves WMI, it is critical to study disease mechanisms and potential therapies in animal models that have similar proportions of white matter compared to humans. However, few small animal species currently used to model preterm brain injury have structural similarities to the human brain.

The ferret (*Mustela putorius furo*) is an attractive species in which to model preterm brain injury because, like preterm human infants (and unlike rodents), they are born lissencephalic and develop gyrencephalic brains postnatally (Empie et al., 2015; Reillo and Borrell, 2012; Barnette et al., 2009). Postnatal white matter maturation and complex cortical folding in newborn ferrets also occur in a similar pattern to that observed in the human brain during the third trimester, which includes the development of the cortical subplate (a transient scaffold for the evolving cortex) that is prominent in human brain development, but minimal in rodents (Callaway and Lieber, 1996; Noctor et al., 1997; Smith and Thompson, 1999). Ferret brain development at birth is roughly equivalent to a 13-week human fetus, while postnatal day (P) 10 and P21 correspond to approximately 24–26 weeks and term gestation in humans, respectively (Empie et al., 2015; Barnette et al., 2009; Sawada and Watanabe, 2012).

The aim of this study was to characterize the ontogeny of white matter and motor skills in the newborn ferret, as well as to determine the distribution of TLRs thought to be important in the etiology of encephalopathy of prematurity, in order to define an appropriate age at which to develop an experimental ferret model of premature WMI in the ferret.

2. Methods

2.1. Animals

Time-mated pregnant jills were acquired from Marshall BioResources (North Rose, NY, USA) at or before day 28 of gestation, and allowed to kindle naturally (typical gestation 41 days). Animals were maintained in a centralized vivarium, and had *ad libitum* access to food and water before and during experimental procedures. Standard housing ferret conditions included a 16-h light/8-h dark cycle with a room temperature range of 61–72 °F (16–22 °C), humidity of 30–70%, and 10–15 fresh air changes per hour. Procedures were performed in accordance with the NIH Guide for the Care and Use of Laboratory Animals and as part of an approved protocol by the University of Washington Institutional Animal Care and Use Committee.

2.2. Ontogeny of white matter and TLRs in the ferret

Healthy ferret kits were sacrificed on postnatal day (P)1 (n = 3), P5 (n = 3), P10 (n = 3), P15 (n = 3), and P20 (n = 3) and perfusion fixed with 10% neutral buffered formalin (NBF). Subsequently, the brains were removed and immersion fixed in NBF for 48–72 h prior to transfer to 70% EtOH. Sagittal sections of brain were obtained for 3 ferrets at all time points. Sagittal sections of brain were also obtained from three adult female ferrets, and coronal sections through the brain were obtained from one other adult female ferret. Additionally, cross sectional slices of brain at the level of the caudate nucleus, thalamus and hippocampus were obtained for kits at each of the following ages: P5 (n = 1), P15 (n = 1), P21 (n = 1), P40 (n = 3), and P70 (n = 2). For gene expression studies, fresh samples of cortex were obtained at P1 (n = 3), P10 (n = 3), P15 (n = 3), P21 (n = 3) and P40 (n = 3).

2.3. Immunohistochemistry

Immunohistochemistry was performed on formalin fixed paraffin embedded sections using antibodies for TLR3 (monoclonal mouse anti ferret, 1:250 dilution, Clone 40C1285.6, LifeSpan BioSciences, LS-C545), TLR4 (polyclonal rabbit anti ferret, 1:2000 dilution, Novus Biological, NBP2-24538), MBP (monoclonal rat anti ferret, 1:500 dilution, Abcam, AB7349), Iba-1 (1:1500 dilution, WAKO Chemicals USA, catalog number 019-19741), and Olig2 (polyclonal rabbit anti ferret, 1:500 dilution, Millipore, Cat No. AB9610). More details are presented in supplemental methods.

2.4. Polymerase chain reaction

Total RNA from brain tissues was isolated according to the manufacturer's instructions, using the QIAGEN RNeasy mini kit (QIAGEN; Valencia, CA). First-strand cDNA was synthesized from equal amount of total RNA by quantitative reverse transcriptase kit (QuantiTect, QIAGEN; Valencia, CA) using the manufacturer's protocol. Real time PCR reaction was conducted on Quantstudio 6 flex instrument (Applied Biosystem, CA). Reactions were carried out using Power Up SYBR green mix (Applied Biosystem, CA). Gene expression of candidate genes and Glyceraldehyde-3-phosphate dehydrogenase (GAPDH; Supplementary Table 1) was measured using qPCR quantitative analysis. All samples were run in triplicate. Relative gene expression between P1 kits and animals of other ages were calculated by using the $2^{-\Delta\Delta Ct}$ method, in which comparative cycle threshold (*Ct)* indicates the fractional cycle number at which the fluorescent signal reaches the detection threshold (Livak and Schmittgen, 2001). Normalized mRNA levels were expressed as x-fold of levels in P1 tissues. Delta *Ct* (ΔCt) was calculated as the difference in *Ct* values for the target genes compared to GAPDH. To obtain absolute quantification of TLR 4 and TLR 3 in ferrets at different ages, TLR4 and TLR 3 primers were validated by generating standard curve. Custom TLR4 and TLR3 gblock fragment (DsDNA amplicon with known copy number) were obtained from IDTDNA, CA. Manufacture protocol was used to prepare the amplicon to obtain absolute gene quantification. To identify absolute copy number of gene at each age group, standard curve was generated with g-block with 1:10 dilution. The cycle threshold (Ct) of each sample group in triplicate were plotted against the standard curve to obtain the copy number of genes at each age group.

2.5. Behavioral testing

Early behavioral tests were performed 3x/week from P21–P42 (n = 5–9 per time point), adapted from routine behavioral tests frequently used in developing rodents, including negative geotaxis (NG), cliff aversion (CA), and spontaneous righting and walking (righting reflex, RR) (Hobbs et al., 2008). The development of NG and RR over time has previously been reported in the juvenile ferret (Christensson and Garwicz, 2005). NG was performed on an inclined plane at 35°. Kits were placed head-down in the middle of the plane, and time to rotate 90° and 180° was recorded. For CA, kits were placed with both front paws on the edge of a shelf. Time to spontaneously retreat away from the edge and rotate away was recorded. In the RR, animals were placed on their backs, and time to righting recorded. From P35 onwards, animals were required to show full foot placement and begin coordinated locomotion in order to complete the righting task. A total of three runs in the NG and CA tests, and five runs of the RR test, were compiled to create an overall behavioral score (Table 1). For all tests, failure was considered to be an inability to complete the task within 60 s. From P42–P70, healthy kits (n = 7) underwent weekly catwalk gait analysis (Catwalk XT, Noldus, Leesburg, VA). At each time point, three compliant runs (lasting < 10 s, maximum speed variation 60%) were collected from each animal. Paw placement, paw width, stride length, speed, and base of support were analyzed over time as measures of early gait development.

2.6. Lipopolysaccharide administration (LPS)

Postnatal day 9 kits (n = 6) received intraperitoneally-administered LPS (Escherichia coli O111:B4, List Biological, CA) at a dose of 1 mg/kg every 12 h for 3 doses. After the last dose of LPS, kits were exposed to hypoxia (6% oxygen for 45 min) followed by hyperoxia (100% oxygen for 6 h). Control animals (n = 4) received equal volume saline injections and normoxia. Kits were sacrificed at P12.

2.7. Statistics

Statistics and images were generated in Prism GraphPad version 7 (San Diego, California). For PCR analyses of TLR3 and TLR4 gene expression, three animals per time point were used for P1, P10, P21, P40, and adult. For PCR analyses of MBP, NG2, PDGFRα, and Olig2, three animals per time point were used for P1, P10, P15, P21, and P40. All samples were run in triplicate. PCR data was log transformed and analyzed by one-way ANOVA followed by direct comparisons between each age and P1 (TLR, NG2, PDGFRα, and Olig2), or for all possible comparisons (MBP). Catwalk data was analyzed by one-way ANOVA followed by comparison of each subsequent time point to the first time point (P42). Bonferroni corrections were used for all multiple comparisons. For histology analyses and for PCR analysis of TLR4 gene expression in kits exposed to LPS and hypoxia/hyperoxia versus control animals, comparisons between LPS-exposed animals and controls were performed using a Mann-Whitney test. For quantitative immunohistochemistry analyses, the ratio of positive staining to total tissue area was calculated for each animal and the mean value was calculated by group. Statistical results with a p-value < 0.05 were considered statistically significant.

3. Results

3.1. Development of pre-oligodendrocyte and mature white matter markers corresponds with early behavioral testing

Relative mRNA expression for PGFRα and NG2, markers for oligodendrocyte precursor cells, was lower at P1 than at other neonatal ages (Fig. 1). Relative mRNA expression for PDGFRα was significantly higher at P10 than P1 ($p = 0.04$), and then decreased at subsequent ages. Relative mRNA expression for NG2 also increased significantly from P1 to P10 ($p = 0.04$), and then remained significantly elevated at approximately the same level through development. Relative mRNA expression of Olig2, a pan-oligodendrocyte marker/transcription factor, peaked at P15 ($p = 0.02$ compared to P1) and then declined (Fig. 1). Olig2 immunohistochemistry performed on coronal sections at the level of the caudate nucleus, corona radiata, and corpus callosum ($n = 1$ per age) showed increased intensity of intranuclear immunopositive staining in the internal capsule and corpus callosum from P5 to P15, followed by subjectively decreased intensity of staining at P21 through P40, with an increased number of immunopositive cells at P70 and a slight increase in staining intensity from P40 through adult (Fig. 1). There was a significant increase in immunopositive staining and relative mRNA expression of MBP throughout neonatal development (Fig. 2), which corresponded with an increase in the mean (range) composite behavioral score (maximum = 13), from 1.6 (1.0–2.3) at P21 to 12.4 (11.3–13.0) at P42 (Fig. 2; $n = 5–9$ per time point). Variability in behavioral score was greatest at P30, with a range of 1.3–10.3 (mean 5.7), and variability also decreased with increasing age. MBP staining performed on coronal sections at the level of the thalamus, hippocampus, and corpus callosum showed essentially absent staining at P5 (Fig. 2). At P15, scattered positive cells were present in the corpus callosum and corona radiata. At P21, there was an increase in positive cells within the corona radiata and corpus callosum, which further dramatically increased at P40 (Fig. 2).

3.2. Characterization of gait development in the ferret

P42 was the earliest age at which kits could successfully ambulate along the length of the catwalk. Over time, mean (SD) speed during completion of the catwalk tended to increase; from 43.3 (16.0) cm/s at P42 to 57.9 (25.7) cm/s at P70 (Fig. 3A). Average print position, a measure of the offset distance between successive footprints decreased over time, and became less variable, from a mean (SD) of 8.1 (6.7) mm/ g at P42 to 0.7 (1.1) mm/g at P63, which was significantly different ($p = 0.009$; Fig. 3B). This suggests that accuracy of paw placement increased over that time period. At P42, mean (SD) forelimb stride length was 16.3 (1.8) cm, which increased to 21.9 (4.6) cm at P70. At the same time, forelimb stride length decreased significantly from 32.3 (4.1) cm at P42 to 18.6 (3.5) cm at P56 ($p < 0.0001$), after which forelimb and hindlimb stride lengths were matched (Fig. 3C). Relative mean forelimb:hindlimb base of support (ratio of the width of placement of the forelimbs compared to the hindlimbs) increased over time, from 0.58 (0.12) at P42 to 0.95 (0.32) at P63, which was statistically significant ($p = 0.04$; Fig. 3D). Both fore and hind paw width also increased significantly from 2.3 (0.2) and 1.8 (0.2) cm, respectively, at P42 to 2.7 (0.2) and 2.3 (0.3) cm at P56 ($p = 0.004$ and $p = 0.01$, respectively), after which they remained similar (Fig. 3E). As both males ($n = 3$) and females ($n = 4$) continued to gain weight after P56 (Fig. 3F), this suggests that paw growth stops at or around P56, after which the body

continues to grow. The largest increases in weight occurred between P38 and P42, when food for the kits was made available at the entrance to the nest, and between P49 and P56, when kits were developed enough to leave the nest fully to gain access to food.

3.3. TLR3 and TLR4 gene expression is present at low levels in the neonatal ferret brain and TLR3 copy number significantly increases from P1 to P40

TLR4 gene expression was present in the neonatal ferret brain from P1–P40, with relative gene expression that was approximately 2 times lower at P1 and P10 than at the later neonatal and adult ages, and with a statistically significant increase from P1to P40 ($p = 0.02$, Fig. 4A). TLR3 gene expression also was present in the neonatal ferret brain from P1–P40, and relative TLR3 expression increased significantly between P1 and P21, and remained significantly elevated into adulthood ($p < 0.01$ for all, Fig. 4B).

TLR4 immunohistochemistry of sagittal and coronal brain sections revealed little immunopositive staining. On TLR4 immunohistochemistry at P1 and P5, very little overall positive staining was noted although there was some positive staining of the olfactory lobe neurons and TLR4 positive epithelium within the choroid plexus with nonspecific staining. At P15, P21, P40 and adults, Purkinje cells of the cerebellum also were mildly-to-moderately positive although non-specific staining especially in the adult samples complicated assessment. At the later ages, weak immunostaining of the epithelium of the choroid plexus also was observed. At all ages, scattered populations of TLR4 positive neurons within the medulla and to a lesser extent the cortex were seen, and virtually no positive staining was observed within white matter.

Immunohistochemistry also revealed very little TLR3 immunopositive staining in the brain during ferret brain development. Occasional positively stained neurons and rare positively stained cells in the periventricular area and the meninges were observed. In the later ages and adult brains, rare neurons and glial cells were positive for TLR3, with perinuclear expression, and some endothelial cells within cerebral blood vessels and within blood vessels of the choroid plexus also were immunopositive.

3.4. LPS plus hypoxia/hyperoxia at P9–10 induces an acute inflammatory response in ferrets

After confirming the presence of early white matter markers at P10, and considering the previous work suggesting that brain development in the P10 ferret most closely resembles that of the 25-week gestation human infant (Barnette et al., 2009), a decision was made to expose kits at P9 to three doses of 1 mg/kg LPS every 12 h followed by hypoxia (6% for 45 min) and hyperoxia (100% for 6 h) at P10. Following this insult, there was no significant difference in TLR4 gene expression (mean ΔCt value; range) within the cortex between exposed (9.84; 8.78–10.64, n = 6) and control (10.36; 10.13–10.75, n = 4) animals at P12 ($p = 0.35$), although TLR4-positive leukocytes were observed within meningeal vessels and expanding the meninges (Fig. 4C–D). There also was no significant difference between Olig2 gene expression (mean ΔCt value; range) within the cortex between exposed (10.29; 9.86–11.18, n = 6)) and control (n = 5; mean ΔCt value = 10.08; range 9.75–10.43) animals at P12 ($p = 0.54$). Histology performed at P12 revealed inflammatory cells including

neutrophils expanding the meninges, and to a lesser degree mildly infiltrating the brain parenchyma (predominantly the cortex), in exposed animals (Fig. 5A–B). The median meningeal inflammation score of exposed animals was 2.5 (range 1–4), compared to 0 (range 0–1) in controls, and this difference was statistically significant ($p = 0.02$). The median parenchymal inflammation score of exposed animals was 1.5 (range 0–2), compared to 0 (range 0–1) in controls, although this difference was not statistically significant ($p = 0.16$). Quantitative analysis of percent positive Iba-1 staining (median; IQR) in exposed animals (0.044; 0.037–0.047, $n = 5$) was significantly greater than in control animals (0.020; 0.017–0.033, $n = 4$) at P12 ($p = 0.03$; Fig. 5C–E). Percent positive GFAP expression (median; IQR) on quantitative immunohistochemistry of sagittal images of the whole brain at P12 in exposed (0.144; 0.093–0.156, $n = 5$) and control animals (0.104; 0.057–0.141) was similar ($p = 0.28$). In the cerebral cortex, median (IQR) percent positive GFAP expression in exposed animals (0.014; 0.008–0.021, $n = 5$) was more than double that seen in controls (0.006; IQR 0.003–0.011, $n = 4$), but the difference was not statistically significant ($p = 0.19$; Fig. 5F). No significant difference in percent positive Olig2 expression in the cerebral cortex between LPS-exposed and control animals at this time point was seen on quantitative immunohistochemistry (data not shown).

4. Discussion

Animal models of neonatal encephalopathy are needed to elucidate pathophysiologic mechanisms of injury and to create a platform for the development and testing of therapeutic interventions. Current rodent models include the Vannucci model of unilateral hypoxic-ischemic brain injury, middle cerebral artery occlusion (MCAO), acute or chronic hypoxia models, and chronic hyperoxia models (Back and Rosenberg, 2014; Back, 2014; Rice et al., 1981; Ashwal et al., 1995; Salmaso et al., 2012; Schwartz et al., 2004). However, these models do not optimally recapitulate human pathological findings, such as the WMI seen in encephalopathy of prematurity. Large animal models such as piglets (Kyng et al., 2015), sheep (Back, 2014; Back et al., 2012), and non-human primates (Traudt et al., 2013) benefit from greater similarities in development to that of human gestation. They also display neonatal and postnatal central nervous system development, white matter: gray matter ratios, and a spectrum of WMI similar to humans. However, development of premature brain injury models in piglets and non-human primates has been unsuccessful to date. Ferrets are attractive as a small animal model species for neonatal encephalopathy because, as with premature human infants in the third trimester, they are lissen-cephalic at birth and subsequently undergo complex cortical folding in the first three weeks of life (Empie et al., 2015; Reillo and Borrell, 2012; Barnette et al., 2009). White matter maturation and synaptogenesis during the early postnatal period in ferrets also mimics development seen during the second half of human gestation (Empie et al., 2015). We undertook this study to further characterize white matter development and TLR ontogeny in the ferret to further inform time points at which the neonatal ferret brain may be most susceptible and vulnerable to injury with LPS and hypoxia/hyperoxia.

Oligodendrocytes are responsible for myelination of the brain and mature oligodendrocytes (OL) derive from oligodendrocyte precursor cells (OPC) (Domingues et al., 2016). Four stages are recognized in oligodendrocyte maturation, from the OPC to the pre-OL (both pre-

myelinating) to the immature OL and mature OL (both myelinating) (2). Infants are most vulnerable to injury of the pre-myelinating pre-OL cells at 23–32 weeks post conceptual age, which corresponds to approximately P10–21 in the ferret (Scafidi et al., 2009; Barnette et al., 2009). Oligodendrocyte precursor cells and pre-oligodendrocytes express PDGFRα and NG2 (Domingues et al., 2016; Wilson et al., 2006) while mature oligodendrocytes express MBP (Back and Rosenberg, 2014; Wright et al., 2010). Olig2 has been shown to be expressed across the oligodendrocyte lineage (Cai et al., 2012). During rodent development, it has been shown that there is a decrease in PDGFRα-expressing oligodendrocyte progenitors with a coincident increase in MBP-expressing mature oligodendrocytes, and by Western blot PDGFRα proteins are highest at P7 and then decline (Wright et al., 2010; He et al., 2009). Similarly, in our study, we found that PDGFRα relative mRNA expression in the ferret was highest at P10 and then declined, Olig2 expression peaked at P15, and MBP relative mRNA expression increased from P10 to P40. Previous rodent studies have found a peak in NG2 positive cells and proteins at P7 in the rat, which is relatively more developed (equivalent gestational age of 32–36 weeks) than the P10 ferret (roughly 23 weeks) (Cai et al., 2012; Chen et al., 2008). We found a significant increase from P0 to P10, although subsequently a similar level of expression persisted until P40. NG2 cells may also give rise to neurons and astrocytes as well as oligodendrocytes (Nishiyama et al., 2009).

In parallel to the development of white matter in ferret kits, we describe an early behavioral test battery (negative geotaxis, cliff aversion, righting), with kits rapidly developing innate reflexes from P28 to P42. From P42 to P70, we have also characterized the gait development of ferrets in a catwalk. The majority of changes (average print position, stride length, paw width, and base of support) occurred between P42 and P56 or P63. The fact that some of the changes reversed slightly at P70 either suggests a further maturation of gait at that time, or could be that the ferrets are too large to freely move within the catwalk (initially designed for rats). Our documented development of early reflexes and gait in healthy P21–P70 ferrets provides an ideal baseline against which to identify deficits or developmental delays caused by an early-life insult.

TLRs are pattern recognition receptors important in the innate immune response that signal as a result of stimulation by a variety of distinct bacterial, viral, or cellular components (Richez et al., 2011). For example, TLR4 is activated by the LPS component of gram negative bacteria, and TLR3 recognizes double stranded RNA associated with viral infections (Bsibsi et al., 2012). TLRs are widely expressed throughout the body, and expression of TLR3 and TLR4 has been shown in the brain, both in neurons, glia, and endothelial cells, with altered and increased expression associated with inflammation, oxidative stress, and white matter injury (Bsibsi et al., 2012; Wang et al., 2011; Vontell et al., 2013; Lathia et al., 2008; Leow-Dyke et al., 2012; Buchanan et al., 2010; Tang et al., 2007, 2008; Nagyoszi et al., 2010). TLR3 and TLR4 agonists have been shown to contribute to perinatal and other brain injury (Stridh et al., 2013a, b; Wang et al., 2009), and activation of the TLR4 signaling pathway likely contributes to neuronal death and blood brain barrier compromise in cases of cerebral ischemia (Teng et al., 2009; Hua et al., 2007; Caso et al., 2007). TLRs may also play a role in regulating normal neuronal proliferation and differentiation (Vontell et al., 2013; Buchanan et al., 2010; Rolls et al., 2007; Cameron et al., 2007; Vontell et al., 2015). Developing reparative therapies for neonatal encephalopathy

requires an understanding of the relationship and interaction between inflammation, hypoxia/hyperoxia, and white matter development in injury.

The degree and location of TLR4 and TLR3 expression in normal neonatal ferret brain is not well described in the literature. In swine, TLR4 expression in seen in cortex, cerebellum, hippocampus and hypothalamus, and TLR4 expression has also been demonstrated in rat neurons and mouse primary neuronal cultures, glial cells, human and rodent brain endothelial cells and cell lines, human and rodent microglia, and in immature and mature choroid plexus under physiologic conditions and associated with systemic inflammation (Leow-Dyke et al., 2012; Nagyoszi et al., 2010; Stridh et al., 2013a; Vaure and Liu, 2014; Skipor et al., 2015; Chakravarty and Herkenham, 2005). In immature chickens, TLR4 expression was observed in the Purkinje cell layer, pia mater, neurons in the medulla and blood vessels in the cerebellum (Ansari et al., 2015). In inflammatory and ischemic CNS disease, TLR4 and TLR3 expression is upregulated in the brain and microglia predominantly express TLR4 (Vontell et al., 2013, 2015; Vaure and Liu, 2014; Ansari et al., 2015). In the present study, TLR4 gene expression increased significantly in the ferret brain from P1 and P10 to the later neonatal and adult ages. This is consistent with a previous study that found lower TLR4 gene expression in P3 and P5 rat brains than at P7–P14 (Vaure and Liu, 2014; Hickey et al., 2011). We found positive TLR4 immunoreactivity in neurons and, to a lesser degree, glial cells in neonatal and adult ferret brains, although some nonspecific and background staining was present. The increase in TLR3 and TLR4 expression from P21 onwards suggests that ferrets may be increasingly susceptible to inflammatory stimuli as they age. As seen in our data, challenges of TLR immunohistochemistry have been previously documented, which include low tissue expression in many tissues and the potential for nonspecific staining (Ungaro et al., 2009).

After confirmation of the presence of early white matter maturational markers and TLRs in the P10 ferret brain, as well as previous work suggesting that the P10 ferret was developmentally most similar to the 25-week gestation human P10 may be the age at which the neonatal ferret is most susceptible to WMI (Barnette et al., 2009). As Olig2 expression peaked at P15, performing an insult at P10 may also result in oligodendrocyte maturational arrest, which is thought to be pathognomonic of premature WMI (Buser et al., 2012; Back, 2015). After LPS administration and hypoxia/hyperoxia at P9–10, inflammatory cells were increased in the meninges, as well as the brain parenchyma, including an increase in TLR4-positive cells. This proof-of-concept work forms the basis for future studies that will include a more sustained inflammation-sensitized hypoxic/hyperoxic insult in the P10 ferret, with relative WMI and motor development determined, and compared to the behavioral testing methods established and presented here.

Our study does have some limitations. Based on the current data, we are unable to ascertain whether LPS exposure, hypoxia, hyperoxia, or their combination, is the most important aspect in the development of an inflammatory response in the neonatal ferret brain. Additionally, though the majority (80%) of exposed animals appeared to have increased GFAP expression compared to controls, suggesting some degree of astrogliosis, this difference was not statistically significant, likely due to the small number of animals in each

group. Similarly, LPS and hypoxia/hyperoxia exposure did not significantly affect Olig2 expression, which may be due to the early time point investigated after the insult.

In summary, our data suggests that the newborn ferret has significant promise as a platform in which to model the neuroinflammation associated with premature birth. Our hope is to develop a ferret model of encephalopathy of prematurity in which to test potential therapeutics before translation to human clinical trials.

Supplementary Material

Refer to Web version on PubMed Central for supplementary material.

References

Ansari AR, Wen L, Huang HB, Wang JX, Huang XY, Peng KM, et al. Lipopolysaccharide stimulation upregulated Toll-like receptor 4 expression in chicken cerebellum. Vet Immunol Immunopathol. 2015; 166(3–4):145–150. [PubMed: 26049167]

Ashwal S, Cole DJ, Osborne S, Osborne TN, Pearce WJ. A new model of neonatal stroke: reversible middle cerebral artery occlusion in the rat pup. Pediatr Neurol. 1995; 12(3):191–196. [PubMed: 7619184]

Back SA. Perinatal white matter injury: the changing spectrum of pathology and emerging insights into pathogenetic mechanisms. Ment Retard Dev Disabil Res Rev. 2006; 12(2):129–140. [PubMed: 16807910]

Back SA. Cerebral white and gray matter injury in newborns: new insights into pathophysiology and management. Clin Perinatol. 2014; 41(1):1–24. [PubMed: 24524444]

Back SA. Brain injury in the preterm infant: new horizons for pathogenesis and prevention. Pediatr Neurol. 2015; 53(3):185–192. [PubMed: 26302698]

Back SA, Rosenberg PA. Pathophysiology of glia in perinatal white matter injury. Glia. 2014; 62(11): 1790–1815. [PubMed: 24687630]

Back SA, Riddle A, Dean J, Hohimer AR. The instrumented fetal sheep as a model of cerebral white matter injury in the premature infant. Neurother: J Am Soc For Exp NeuroTher. 2012; 9(2):359–370.

Barnette AR, Neil JJ, Kroenke CD, Griffith JL, Epstein AA, Bayly PV, et al. Characterization of brain development in the ferret via MRI. Pediatr Res. 2009; 66(1):80–84. [PubMed: 19287340]

Brehmer F, Bendix I, Prager S, van de Looij Y, Reinboth BS, Zimmermanns J, et al. Interaction of inflammation and hyperoxia in a rat model of neonatal white matter damage. PLoS One. 2012; 7(11):e49023. [PubMed: 23155446]

Bsibsi M, Nomden A, van Noort JM, Baron W. Toll-like receptors 2 and 3 agonists differentially affect oligodendrocyte survival, differentiation, and myelin membrane formation. J Neurosci Res. 2012; 90(2):388–398. [PubMed: 21971760]

Buchanan MM, Hutchinson M, Watkins LR, Yin H. Toll-like receptor 4 in CNS pathologies. J Neurochem. 2010; 114(1):13–27. [PubMed: 20402965]

Buser JR, Maire J, Riddle A, Gong X, Nguyen T, Nelson K, et al. Arrested preoligodendrocyte maturation contributes to myelination failure in premature infants. Ann Neurol. 2012; 71(1):93–109. [PubMed: 22275256]

Cai J, Tuong CM, Zhang Y, Shields CB, Guo G, Fu H, et al. Mouse intermittent hypoxia mimicking apnoea of prematurity: effects on myelinogenesis and axonal maturation. J Pathol. 2012; 226(3): 495–508. [PubMed: 21953180]

Callaway EM, Lieber JL. Development of axonal arbors of layer 6 pyramidal neurons in ferret primary visual cortex. J Comp Neurol. 1996; 376(2):295–305. [PubMed: 8951644]

Cameron JS, Alexopoulou L, Sloane JA, DiBernardo AB, Ma Y, Kosaras B, et al. Toll-like receptor 3 is a potent negative regulator of axonal growth in mammals. J Neurosci. 2007; 27(47):13033–13041. [PubMed: 18032677]

Caso JR, Pradillo JM, Hurtado O, Lorenzo P, Moro MA, Lizasoain I. Toll-like receptor 4 is involved in brain damage and inflammation after experimental stroke. Circulation. 2007; 115(12):1599–1608. [PubMed: 17372179]

Chakravarty S, Herkenham M. Toll-like receptor 4 on nonhematopoietic cells sustains CNS inflammation during endotoxemia, independent of systemic cytokines. J Neurosci. 2005; 25(7): 1788–1796. [PubMed: 15716415]

Chen PH, Cai WQ, Wang LY, Deng QY. A morphological and electrophysiological study on the postnatal development of oligodendrocyte precursor cells in the rat brain. Brain Res. 2008; 1243:27–37. [PubMed: 18824157]

Christensson M, Garwicz M. Time course of postnatal motor development in ferrets: ontogenetic and comparative perspectives. Behav Brain Res. 2005; 158(2):231–242. [PubMed: 15698889]

Dean JM, Shi Z, Fleiss B, Gunn KC, Groenendaal F, van Bel F, et al. A critical review of models of perinatal infection. Dev Neurosci. 2015; 37(4–5):289–304. [PubMed: 25720344]

Domingues HS, Portugal CC, Socodato R, Relvas JB. Oligodendrocyte, astrocyte, and microglia crosstalk in myelin development, damage, and repair. Front Cell Dev Biol. 2016; 4:71. [PubMed: 27551677]

Empie K, Rangarajan V, Juul SE. Is the ferret a suitable species for studying perinatal brain injury? Int J Dev Neurosci. 2015; 45:2–10. [PubMed: 26102988]

Hagberg H, Mallard C, Ferriero DM, Vannucci SJ, Levison SW, Vexler ZS, et al. The role of inflammation in perinatal brain injury. Nat Rev Neurol. 2015; 11(4):192–208. [PubMed: 25686754]

He Y, Cai W, Wang L, Chen P. A developmental study on the expression of PDGFalphaR immunoreactive cells in the brain of postnatal rats. Neurosci Res. 2009; 65(3):272–279. [PubMed: 19665498]

Hickey E, Shi H, Van Arsdell G, Askalan R. Lipopolysaccharide-induced preconditioning against ischemic injury is associated with changes in toll-like receptor 4 expression in the rat developing brain. Pediatr Res. 2011; 70(1):10–14. [PubMed: 21659958]

Hobbs C, Thoresen M, Tucker A, Aquilina K, Chakkarapani E, Dingley J. Xenon and hypothermia combine additively, offering long-term functional and histopathologic neuroprotection after neonatal hypoxia/ischemia. Stroke. 2008; 39(4):1307–1313. [PubMed: 18309163]

Hua F, Ma J, Ha T, Xia Y, Kelley J, Williams DL, et al. Activation of Toll-like receptor 4 signaling contributes to hippocampal neuronal death following global cerebral ischemia/reperfusion. J Neuroimmunol. 2007; 190(1–2):101–111. [PubMed: 17884182]

Kyng KJ, Skajaa T, Kerrn-Jespersen S, Andreassen CS, Bennedsgaard K, Henriksen TB. A piglet model of neonatal hypoxic-ischemic encephalopathy. J Vis Exp: JoVE. 2015; 99:e52454.

Lathia JD, Okun E, Tang SC, Griffioen K, Cheng A, Mughal MR, et al. Toll-like receptor 3 is a negative regulator of embryonic neural progenitor cell proliferation. J Neurosci. 2008; 28(51): 13978–13984. [PubMed: 19091986]

Leow-Dyke S, Allen C, Denes A, Nilsson O, Maysami S, Bowie AG, et al. Neuronal Toll-like receptor 4 signaling induces brain endothelial activation and neutrophil transmigration in vitro. J Neuroinflamm. 2012; 9:230.

Livak KJ, Schmittgen TD. Analysis of relative gene expression data using real-time quantitative PCR and the 2(−Delta Delta C(T)) method. Methods. 2001; 25(4):402–408. [PubMed: 11846609]

Nagyoszi P, Wilhelm I, Farkas AE, Fazakas C, Dung NT, Hasko J, et al. Expression and regulation of toll-like receptors in cerebral endothelial cells. Neurochem Int. 2010; 57(5):556–564. [PubMed: 20637248]

Nishiyama A, Komitova M, Suzuki R, Zhu X. Polydendrocytes (NG2 cells): multifunctional cells with lineage plasticity. Nat Rev Neurosci. 2009; 10(1):9–22. [PubMed: 19096367]

Noctor SC, Scholnicoff NJ, Juliano SL. Histogenesis of ferret somatosensory cortex. J Comp Neurol. 1997; 387(2):179–193. [PubMed: 9336222]

Reillo I, Borrell V. Germinal zones in the developing cerebral cortex of ferret: ontogeny, cell cycle kinetics, and diversity of progenitors. Cereb Cortex. 2012; 22(9):2039–2054. [PubMed: 21988826]

Rice JE 3rd, Vannucci RC, Brierley JB. The influence of immaturity on hypoxic-ischemic brain damage in the rat. Ann Neurol. 1981; 9(2):131–141. [PubMed: 7235629]

Richez C, Blanco P, Rifkin I, Moreau JF, Schaeverbeke T. Role for toll-like receptors in autoimmune disease: the example of systemic lupus erythematosus. Jt Bone Spine: revue du rhumatisme. 2011; 78(2):124–130.

Rolls A, Shechter R, London A, Ziv Y, Ronen A, Levy R, et al. Toll-like receptors modulate adult hippocampal neurogenesis. Nat Cell Biol. 2007; 9(9):1081–1088. [PubMed: 17704767]

Salmaso N, Silbereis J, Komitova M, Mitchell P, Chapman K, Ment LR, et al. Environmental enrichment increases the GFAP++ stem cell pool and reverses hypoxia-induced cognitive deficits in juvenile mice. J Neurosci. 2012; 32(26):8930–8939. [PubMed: 22745493]

Sawada K, Watanabe M. Development of cerebral sulci and gyri in ferrets (Mustela putorius). Congenit Anom. 2012; 52(3):168–175.

Scafidi J, Fagel DM, Ment LR, Vaccarino FM. Modeling premature brain injury and recovery. Int J Dev Neurosci. 2009; 27(8):863–871. [PubMed: 19482072]

Schwartz ML, Vaccarino F, Chacon M, Yan WL, Ment LR, Stewart WB. Chronic neonatal hypoxia leads to long term decreases in the volume and cell number of the rat cerebral cortex. Semin Perinatol. 2004; 28(6):379–388. [PubMed: 15693394]

Skipor J, Szczepkowska A, Kowalewska M, Herman AP, Lisiewski P. Profile of toll-like receptor mRNA expression in the choroid plexus in adult ewes. Acta Vet Hung. 2015; 63(1):69–78. [PubMed: 25374259]

Smith AL, Thompson ID. Spatiotemporal patterning of glutamate receptors in developing ferret striate cortex. Eur J Neurosci. 1999; 11(3):923–934. [PubMed: 10103086]

Stridh L, Ek CJ, Wang X, Nilsson H, Mallard C. Regulation of Toll-like receptors in the choroid plexus in the immature brain after systemic inflammatory stimuli. Transl Stroke Res. 2013a; 4(2):220–227. [PubMed: 23741282]

Stridh L, Mottahedin A, Johansson ME, Valdez RC, Northington F, Wang X, et al. Toll-like receptor-3 activation increases the vulnerability of the neonatal brain to hypoxia-ischemia. J Neurosci. 2013b; 33(29):12041–12051. [PubMed: 23864690]

Tang SC, Arumugam TV, Xu X, Cheng A, Mughal MR, Jo DG, et al. Pivotal role for neuronal Toll-like receptors in ischemic brain injury and functional deficits. Proc Natl Acad Sci U S A. 2007; 104(34):13798–13803. [PubMed: 17693552]

Tang SC, Lathia JD, Selvaraj PK, Jo DG, Mughal MR, Cheng A, et al. Toll-like receptor-4 mediates neuronal apoptosis induced by amyloid beta-peptide and the membrane lipid peroxidation product 4-hydroxynonenal. Exp Neurol. 2008; 213(1):114–121. [PubMed: 18586243]

Teng W, Wang L, Xue W, Guan C. Activation of TLR4-mediated NFkappaB signaling in hemorrhagic brain in rats. Mediators Inflamm. 2009; 2009:473276. [PubMed: 20150961]

Thomson CA, McColl A, Cavanagh J, Graham GJ. Peripheral inflammation is associated with remote global gene expression changes in the brain. J Neuroinflamm. 2014; 11:73.

Traudt CM, McPherson RJ, Bauer LA, Richards TL, Burbacher TM, McAdams RM, et al. Concurrent erythropoietin and hypothermia treatment improve outcomes in a term nonhuman primate model of perinatal asphyxia. Dev Neurosci. 2013; 35(6):491–503. [PubMed: 24192275]

Ungaro R, Abreu MT, Fukata M. Practical techniques for detection of Toll-like receptor-4 in the human intestine. Methods Mol Biol. 2009; 517:345–361. [PubMed: 19378023]

Vaure C, Liu Y. A comparative review of toll-like receptor 4 expression and functionality in different animal species. Front Immunol. 2014; 5:316. [PubMed: 25071777]

Volpe JJ. Brain injury in premature infants: a complex amalgam of destructive and developmental disturbances. Lancet Neurol. 2009; 8(1):110–124. [PubMed: 19081519]

Vontell R, Supramaniam V, Thornton C, Wyatt-Ashmead J, Mallard C, Gressens P, et al. Toll-like receptor 3 expression in glia and neurons alters in response to white matter injury in preterm infants. Dev Neurosci. 2013; 35(2–3):130–139. [PubMed: 23548575]

Vontell R, Supramaniam V, Wyatt-Ashmead J, Gressens P, Rutherford M, Hagberg H, et al. Cellular mechanisms of toll-like receptor-3 activation in the thalamus are associated with white matter

injury in the developing brain. J Neuropathol Exp Neurol. 2015; 74(3):273–285. [PubMed: 25668563]

Wang YC, Lin S, Yang QW. Toll-like receptors in cerebral ischemic inflammatory injury. J Neuroinflamm. 2011; 8:134.

Wang X, Stridh L, Li W, Dean J, Elmgren A, Gan L, et al. Lipopolysaccharide sensitizes neonatal hypoxic-ischemic brain injury in a MyD88-dependent manner. J Immunol. 2009; 183(11):7471–7477. [PubMed: 19917690]

Wilson HC, Scolding NJ, Raine CS. Co-expression of PDGF alpha receptor and NG2 by oligodendrocyte precursors in human CNS and multiple sclerosis lesions. J Neuroimmunol. 2006; 176(1–2):162–173. [PubMed: 16753227]

Wright J, Zhang G, Yu TS, Kernie SG. Age-related changes in the oligodendrocyte progenitor pool influence brain remodeling after injury. Dev Neurosci. 2010; 32(5–6):499–509. [PubMed: 21160162]

Appendix A. Supplementary data

Supplementary material related to this article can be found, in the online version, at doi: https://doi.org/10.1016/j.ijdevneu.2018.05.006.

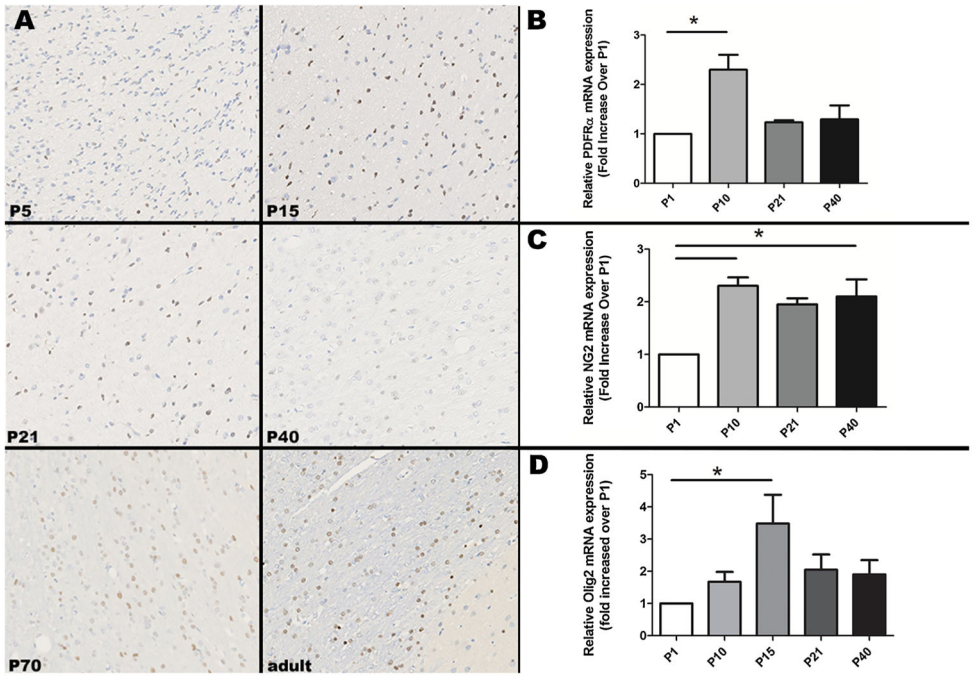

Fig. 1.

(A) In the internal capsule at the level of the caudate nucleus, Olig2 immunohistochemistry shows increased intensity of staining at P15 relative to P5, with less intense but more numerous immunopositive cells in the P70 and adult animals. Olig2 positive cells are brown; hematoxylin counterstain. Original magnification is 20 ×. (B) Relative PDGFRα mRNA expression from P1 to P40 shows a significant increase from P1 to P10. (C) Relative NG2 mRNA expression from P1 to P40 shows a significant increase from P1 to P10 and P40. (D) Relative Olig2 mRNA expression from P1 to P40 shows a significant increase from P1 to P15. Asterisks indicate $p < 0.05$.

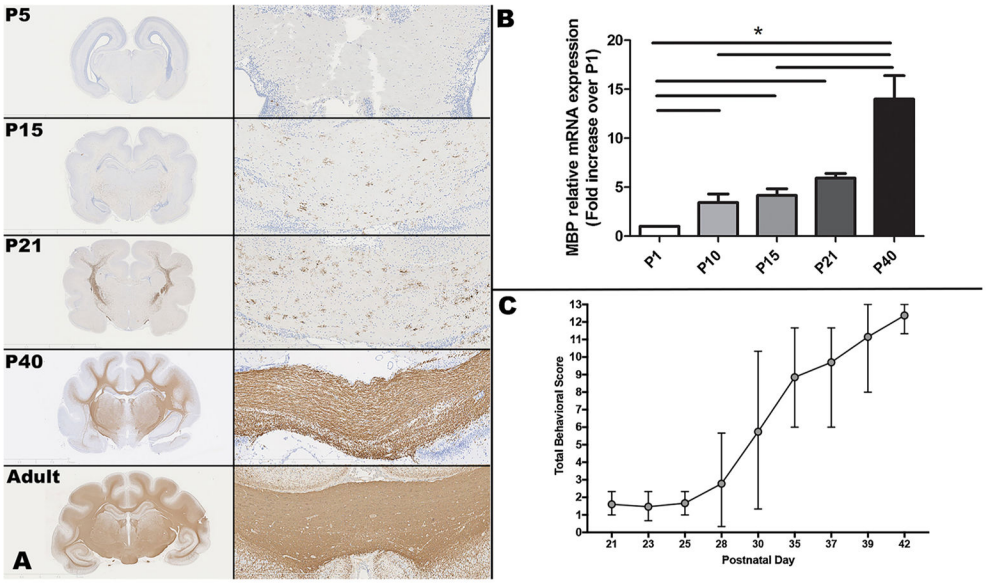

Fig. 2.

(A) Myelin basic protein (MBP) immunoreactivity (brown staining) increases dramatically over time in from the P5 to adult ferret. Images on the left show a lower magnification view of the brain at the level of the thalamus and hippocampus; the images on the right show a 10X origination magnification view of the corpus callosum. MBP positive cells are brown; hematoxylin counterstain. (B) MBP relative mRNA expression also increases significantly over time, with a > 2-fold increase from P21 to P40. (C) Total behavioral scores increase in a similar fashion from P21 to P40. Asterisks indicate $p < 0.05$.

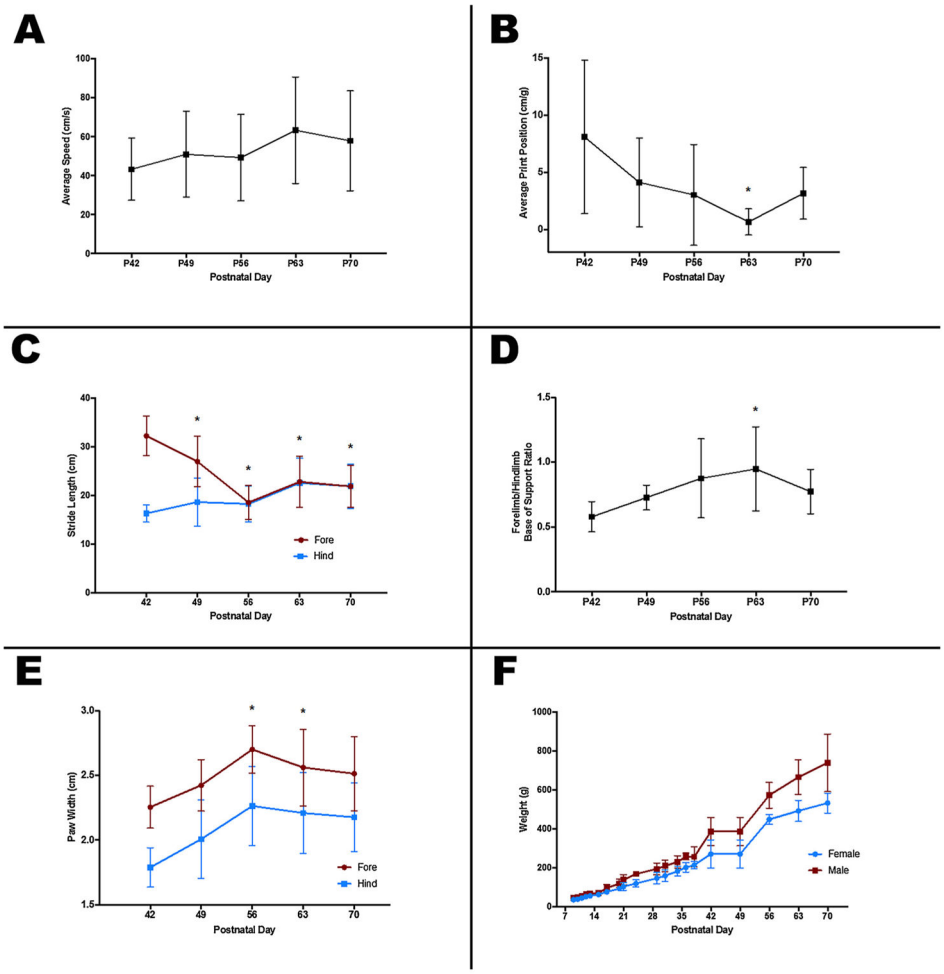

Fig. 3.

Gait development and weight gain in the ferret. Average speed on the catwalk (A) tended to increase over time, but not significantly. Relative distance between successive paw placements (B) decreased, and became less variable, with age. Average forelimb and hindlimb stride length over time (C) shows that forelimb stride length decreases over time to match hindlimb stride length by P56. Relative width of forelimb and hindlimb base of support (D) increased over time, peaking at P63. Fore and hind paw widths (E) also increased over time, reaching their full size around P56, while body weight continued to increase (F). Asterisks indicate $p < 0.05$ compared to P42 values.

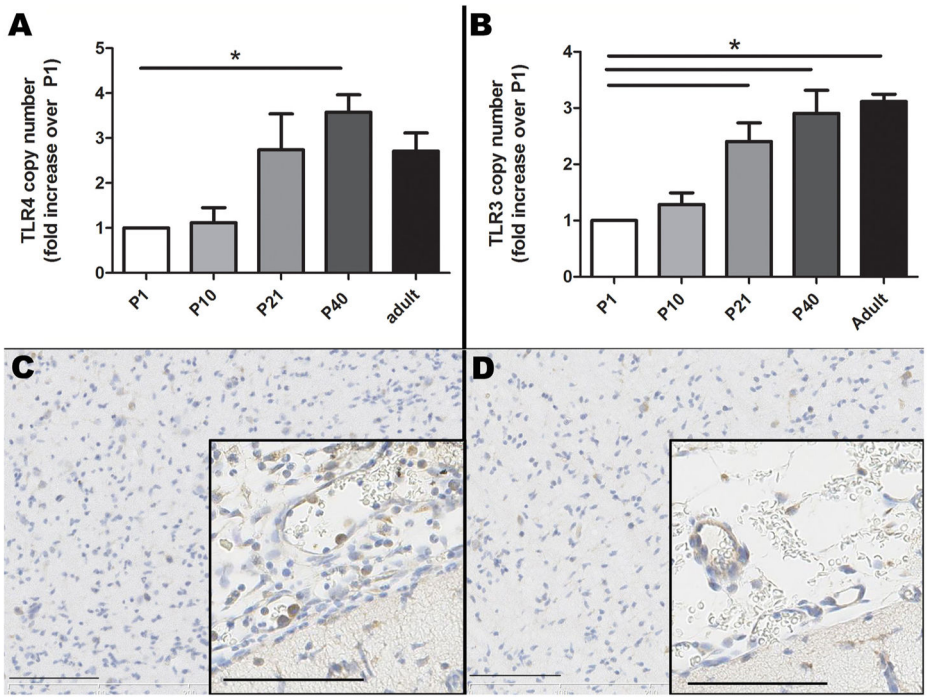

Fig. 4.

TLR4 (A) and TLR3 (B) relative mRNA expression is present at low levels in the neonatal ferret brain, and significantly increases from P1 to P40. P12 ferrets exposed to 1 mg/kg LPS x 3 doses + hypoxia/hyperoxia have increased TLR4 immunopositive cells within meningeal vessels and expanding the meninges (C), relative to controls (saline followed by normoxia) (D). TLR4 positive cells are brown; hematoxylin counterstain; bars = 100 μm. Asterisks indicate $p < 0.05$.

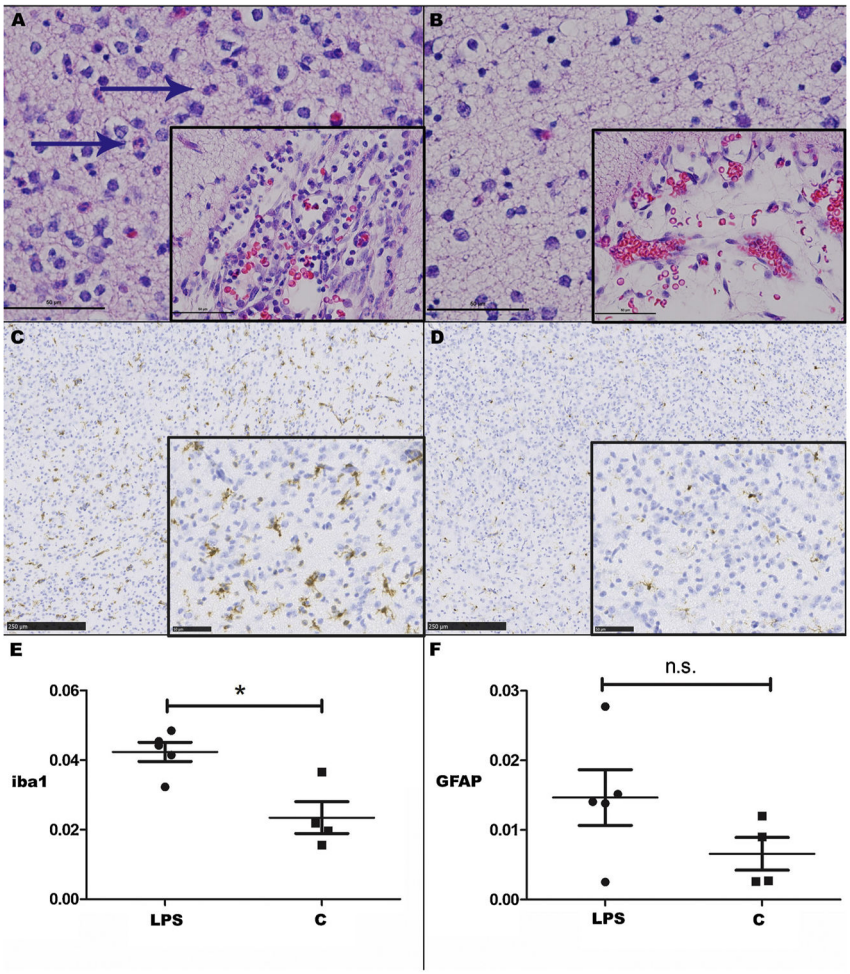

Fig. 5.

(A) P12 ferrets exposed to 1 mg/kg LPS x 3 doses + hypoxia/hyperoxia at P9–10 have increased inflammation within the meninges and neuropil compared to controls (B). Hematoxylin and eosin (HE), bar = 50 μm (inset bar = 50 μm). Neutrophils are indicated by blue arrows. (C) Iba-1 positive staining at P12 in exposed animals is increased compared to controls (D, E). Iba-1 positive cells are brown, hematoxylin counterstain. Bar = 250 μm (inset bar = 50 μm). (F) There is no significant difference in the cerebral cortex on GFAP staining. Asterisks indicate $p < 0.05$; n.s.=not significant. (For interpretation of the references to colour in this figure legend, the reader is referred to the web version of this article).

Table 1

Scoring system used for early behavioural testing (P21–P42).

Test	Runs	Scoring
Negative Geotaxis	3	1 = Stayed on plane (did not fall). 2 = Rotated 90 degrees. 3 = Rotated 180 degrees (with time). Score averaged from 3 runs (maximum score of 3).
Cliff Aversion	3	1 = Fell. 2 = Rotated head away from ledge. 3 = Rotated whole upper body away from ledge. 4 = Upper body actively moved away from ledge. 5 = Full rotation and active locomotion away from ledge. Average score from 3 runs (maximum score of 5).
Righting reflex	5	1 point for each completion (maximum score of 5).
Maximum Total Score	13	